Maize yields over Europe may increase in spite of climate change, with an appropriate use of the genetic variability of flowering time

Boris Parent[a], Margot Leclere[a,1], Sébastien Lacube[a], Mikhail A. Semenov[b], Claude Welcker[a], Pierre Martre[a], and François Tardieu[a,2]

[a]Laboratoire d'Ecophysiologie des Plantes sous Stress Environnementaux (LEPSE), Université de Montpellier, Institut National de la Recherche Agronomique (INRA), F-34000 Montpellier, France; and [b]Plant Sciences Department, Rothamsted Research, Harpenden, AL5 2JQ Herts, United Kingdom

Edited by Edward S. Buckler, USDA-ARS/Cornell University, Ithaca, NY, and approved August 24, 2018 (received for review December 3, 2017)

Projections based on invariant genotypes and agronomic practices indicate that climate change will largely decrease crop yields. The comparatively few studies considering farmers' adaptation result in a diversity of impacts depending on their assumptions. We combined experiments and process-based modeling for analyzing the consequences of climate change on European maize yields if farmers made the best use of the current genetic variability of cycle duration, based on practices they currently use. We first showed that the genetic variability of maize flowering time is sufficient for identifying a cycle duration that maximizes yield in a range of European climatic conditions. This was observed in six field experiments with a panel of 121 accessions and extended to 59 European sites over 36 years with a crop model. The assumption that farmers use optimal cycle duration and sowing date was supported by comparison with historical data. Simulations were then carried out for 2050 with 3 million combinations of crop cycle durations, climate scenarios, management practices, and modeling hypotheses. Simulated grain production over Europe in 2050 was stable (−1 to +1%) compared with the 1975–2010 baseline period under the hypotheses of unchanged cycle duration, whereas it was increased (+4–7%) when crop cycle duration and sowing dates were optimized in each local environment. The combined effects of climate change and farmer adaptation reduced the yield gradient between south and north of Europe and increased European maize production if farmers continued to make the best use of the genetic variability of crop cycle duration.

climate change | yield | flowering time | management practices | modeling

Most projections relying on process-based (1–5) or statistical models (6) predict that climate change will reduce yields of most crop species. Indeed, crops will experience more heat events, dry weather, and an increase in evaporative demand which may all decrease crop production (6–8). However, some species still show yield progress in farmer's fields despite observed climate changes (9). This discrepancy may be due to the fact that many impact studies assume unchanged farmer's genotypes and practices, whereas farmers continuously adapt crop cycle duration and sowing dates to local environmental conditions (10–12). The comparatively few studies of climate change impact that consider adaptation of management practices (13) predict a decrease in yield by 1–6%, smaller than without adaptation (10–12). Furthermore, a study that considers adaptation of sowing date and cycle duration for six crops predicts a yield increase of 12–16% (14). This diversity of projections led us to develop a more explicit approach based on experiments and process-based modeling and to use a precise definition of adaptation involving biological variables and management practices currently used by farmers.

The duration of crop cycle (*i*) is largely affected by climate change through increase in temperature; (*ii*) has a major effect on crop yield via cumulated canopy photosynthesis; and (*iii*) presents a large genetic variability in most species, in particular via the genetic control of flowering time that involves networks of genes that interact with environmental conditions (15–18). This raises the possibility that farmers can counteract the effects of climate change by making the best use of the genetic variability of flowering time (10, 19), thereby adapting phenology to climate changes as it has been the case over centuries in natural ecosystems (20). This raises the questions of whether (*i*) farmers can access an organized genetic variability of cycle duration to adapt crop cycle to a range of environmental conditions; (*ii*) one can model the decision rules that farmers currently use for adapting cycle duration over environmental gradients, together with sowing dates; and (*iii*) adapting crop cycle duration can counteract the effects of climate change. More specifically, we have questioned whether the decision rules currently used by farmers to adapt crop cycle duration over environmental gradients would reduce the impact of climate change on European maize production.

Addressing these questions required an experimental approach for the first question, a model of farmer's decision rules together with a comparison of model outputs with European statistics for the second question, and a crop simulation model that explicitly accounts for the genetic variability of flowering time and of crop responses to environmental conditions for the third question. We combined multilocation field experiments

Significance

The consequences of climate change on European maize yields may become positive if farmers in 2050 use the decision rules they currently follow for adapting plant cycle duration and sowing dates to the diversity of environmental conditions. Experiments and simulations show that the current genetic variability of flowering time allows identifying a cycle duration that maximizes yield at every maize field in Europe. The assumption that farmers use this optimal cycle length in each site was supported by comparison with historical data. Simulated European production for 2050 was stable under the hypotheses of unchanged practices but was increased if farmers continued adopting the decision rules they currently use for adjusting sowing date and crop cycle duration to local environment.

Author contributions: B.P. and F.T. designed research; B.P., M.L., S.L., M.A.S., C.W., and F.T. performed research; B.P., M.L., S.L., M.A.S., C.W., P.M., and F.T. analyzed data; and B.P., M.A.S., P.M., and F.T. wrote the paper.

The authors declare no conflict of interest.

This article is a PNAS Direct Submission.

[1]Present address: UMR Agronomie, INRA, AgroParisTech, Université Paris-Saclay, 78850 Thiverval-Grignon, France.

[2]To whom correspondence should be addressed. Email: francois.tardieu@inra.fr.

This article contains supporting information online at www.pnas.org/lookup/suppl/doi:10.1073/pnas.1720716115/-/DCSupplemental.

Published online October 1, 2018.

that analyzed the consequences of the genetic variability of crop duration, historical yields, crop management and phenology information, and projections of midterm climate change impacts. These were performed for European maize, whose flowering time is a constitutive trait, depending on temperature but independent of photoperiod sensitivity or cold requirement.

Results

The Existing Genetic Variability of Cycle Duration Allows Optimizing Yield in a Wide Range of Current Environmental Scenarios. We first tested whether the current genetic variability of cycle duration allowed identification of an optimum cycle duration that maximizes grain yield in each site. This was based on six experiments, extended to the variability of climate over Europe via modeling. A panel of 121 maize accessions with a large range of flowering time, due to allelic variations in the VGT1 (18), VGT2 (15), and other loci (16), was analyzed in six experiments with different climatic scenarios and water regimes (Fig. 1*A* and *SI Appendix*, Figs. S1–S3). Because the main source of variation of maize cycle duration is the length of the vegetative phase via the allelic effects of genes involved in flowering time (17, 21), we focus hereafter on the sowing-to-flowering period. For each accession, the duration of this period was common to all sites if expressed in time corrected for temperature (*SI Appendix*, Fig. S1) and closely correlated to leaf number, which itself depends on the time to floral transition (22) (*SI Appendix*, Fig. S2). Accessions with sowing-to-flowering durations that optimize yield were identified in each experiment (Fig. 1*A* and *SI Appendix*, Fig. S3). Yield increased with vegetative duration below this optimum (Fig. 1*A*), because of increased light interception (*SI Appendix*, Fig. S4), and decreased beyond it, due to flowering and/or grain filling occurring in adverse conditions such as low light or terminal drought (23). As expected, different optimum durations were observed among sites and water regimes, depending on local environmental conditions (*SI Appendix*, Fig. S3).

We extended this analysis to 59 European sites representative of the European maize growing area (*SI Appendix*, Table S1) (24). Simulations were performed over 36 y (1975–2010) with a modified version of the crop simulation model Agricultural Production Systems Simulator (APSIM) maize (25), in which vapor pressure deficit (VPD) and, indirectly, high temperature have direct effects on leaf expansion rate and grain set, with calculations run with a 3-h time step. This model also accounts for the genetic variability of phenology by considering the maximum leaf number as a genotypic input for the simulations of cycle duration, individual leaf expansion, and grain abortion (26, 27). Simulations were run for each individual year in either rainfed or irrigated conditions. The mean value of yield over the 36-y period was related to the sowing-to-flowering duration with bell shapes similar to those observed experimentally (Fig. 1*B* and *SI Appendix*, Fig. S5 *A*, *C*, and *E*). In irrigated conditions, optimum durations differed among sites and correlated with latitude (*SI Appendix*, Figs. S2*A* and S6*A*). Simulated optimum crop cycle durations were lower in rainfed than in irrigated conditions, especially in most southern locations in which short crop cycles allowed escaping water deficit during flowering time (Fig. 2*B* and *SI Appendix*, Fig. S6*B*).

Overall, both experiments and simulations showed that optimum cycle durations that maximize yield can be identified based on the genetic variation of flowering time in a wide diversity of environmental scenarios throughout Europe.

A Model of Cycle Duration and Sowing Date Closely Matched with the Management Practices That Farmers Currently Use in the Diversity of Environmental Scenarios. The above paragraphs suggest that, by trial and error, farmers and extension services might identify a cycle duration that maximizes yield in the most frequent climatic scenario corresponding to each site ("autonomous adaptation,"

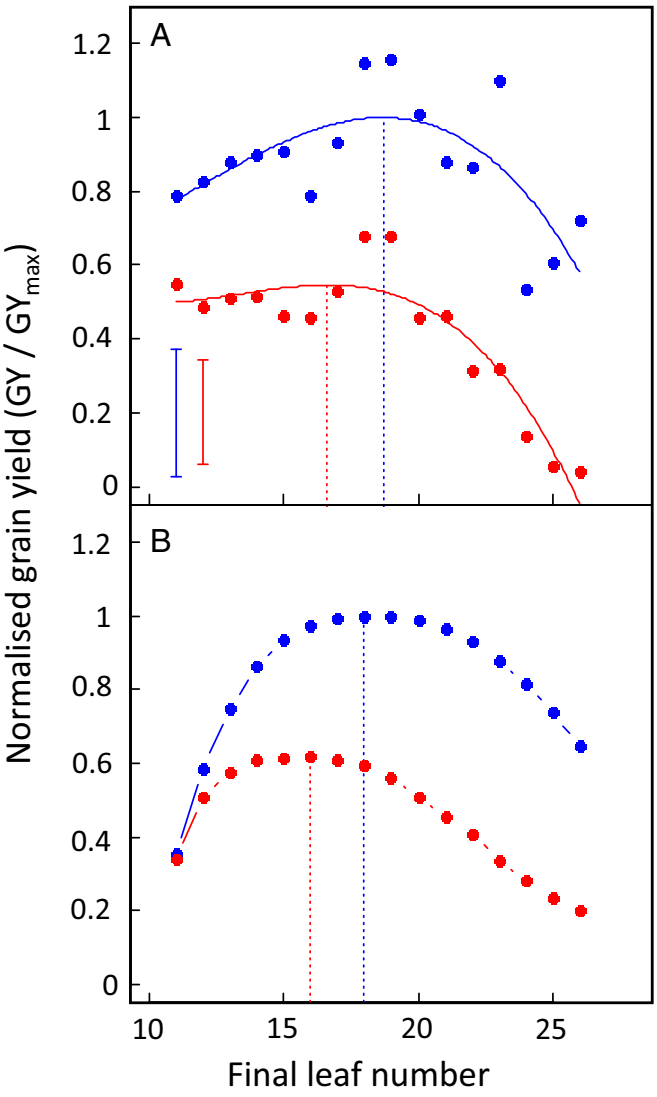

Fig. 1. Observed and simulated optimum durations of the vegetative period (sowing–flowering time), expressed in final plant leaf number. (*A*) Experimental relationships between final plant leaf number and yield in irrigated (blue dots and lines) or rainfed conditions (red dots and line) in a field with 121 maize accessions (two additional field experiments are presented in *SI Appendix*, Fig. S3). For better intuition, the duration of the vegetative period is expressed as final leaf number, closely related to it. Yield is normalized by its maximum value in fully irrigated conditions. Dots are mean values for accessions presenting a common leaf number. Error bars, confidence intervals (P = 0.95). Plain lines, third-order polynomial regressions. Vertical dashed lines, optimum leaf number. (*B*) Simulated relationship between plant leaf number and yield at Achenheim, France (*SI Appendix*, Table S1, two additional sites are presented in *SI Appendix*, Fig. S5). Each dot, mean of 36 y (1975–2010). Error bars, confidence intervals (P = 0.95).

ref. 28). This has allowed us to model their decision rules about cycle duration, but also sowing date, and to compare simulation outputs to farmers' practices reported in European databases (29, 30). The simulation of cycle duration used by farmers at each site was based on the calculated optimum sowing-to-flowering duration presented above. Simulated sowing dates occurred on the first day of early spring for which the risk of frost for 10 d after sowing was lower than 5% over 36 y, thereby combining a minimum risk of plant damage with highest potentials of cumulated photosynthesis and yield. They ranged from March 20 to April 30, with later dates at northern latitudes.

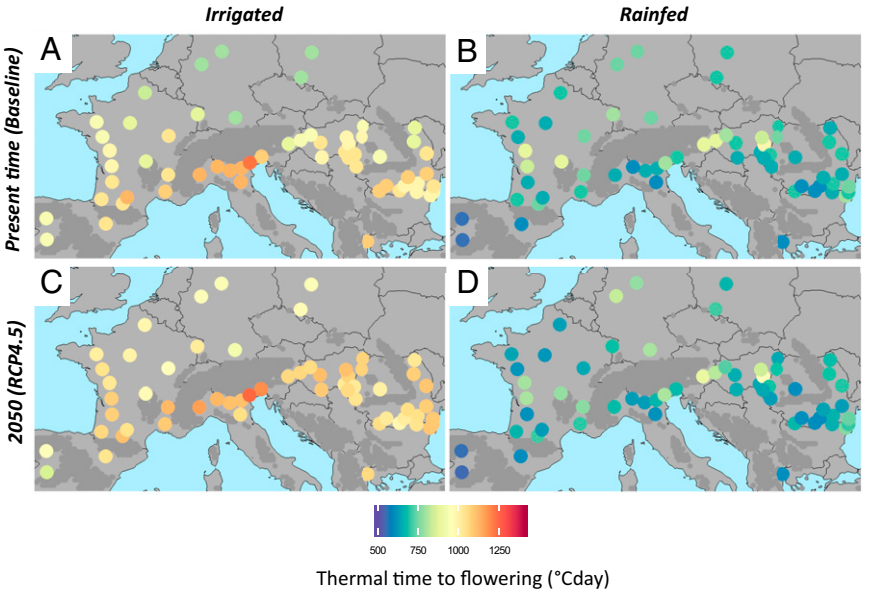

Fig. 2. Maps of optimum cycle duration in current (*A* and *B*) and future conditions (*C* and *D*), under irrigated (*A* and *C*) or rainfed (*B* and *D*). Colors depict the optimum thermal time between sowing and flowering time in each site for maximizing yield for present time (over the 1975–2010 period) or 2050 (30 y, RCP4.5, average duration for six GCMs, calculated under the hypothesis of an increase in transpiration efficiency with CO_2 concentration).

The spatial distribution of sowing dates and flowering times simulated in this way closely matched with those reported in the European AgroPheno database (29) (*SI Appendix*, Fig. S7*A*). Cycle duration decreased with latitude: later sowing dates in northern sites such as Germany or Poland were compensated for by shorter vegetative durations (Fig. 2*A* and *SI Appendix*, Fig. S6*A*), resulting in simulated flowering dates that were nearly independent of latitude in both simulations and historical data (29) (*SI Appendix*, Fig. S7*A*).

Hence, the decision rules simulated as above allowed correct prediction of farmer practices throughout Europe. In addition, simulated yields at country level calculated by using local practices of irrigation, density, and fertilization closely correlated with historical yields for the period 2000–2010 (30) (*SI Appendix*, Fig. S7*B*). To compare environmental effects independently of sowing density and fertilization, simulations were then run by considering a common sowing density over Europe (eight plants m^{-2}) and no nitrogen limitation. In irrigated conditions, simulated yields (9.2–13.6 t ha^{-1}, Fig. 3*A* and *SI Appendix*, Fig. S8) were negatively related to latitude with highest yield in southern sites (Fig. 3*A*); this relationship disappeared in rainfed conditions due to the higher risk of water deficit in southern Europe, so maximum yields were observed at intermediate latitudes 44–47° N (Fig. 3*D* and *SI Appendix*, Fig. S8).

Adapting Crop Cycle Duration Based on Current Farmer's Decision Rules Improved the Simulated Impacts of Climate Change Compared with Invariant Practices. We projected yields for 2050 by considering that the farmer's decision rules presented above, based on the assumption of optimal practices, will apply in the future. We then compared the yields simulated with either adapted or invariant cycle durations and sowing dates. Daily local-scale climate scenarios for 2050 were generated by the Long Ashton Research Station Weather Generator (LARS-WG) (31) for the representative concentration pathways (RCPs) 4.5 and 8.5 (487 and 541 ppm CO_2 in 2050, respectively). For each RCP, we used six global climate models (GCMs) that cover the range and present similar mean values for changes in temperature, VPD, and precipitations compared with 18 GCMs from the Coupled Model Intercomparison Project Phase 5 (CMIP5) model ensemble for the studied area (32) (*SI Appendix*, Fig. S9). Thirty years of daily weather data were generated for each site–RCP–GCM combination. The direct impact of increase in atmospheric CO_2 concentration in 2050 was taken into account in the crop model by increasing transpiration efficiency (TE) by 0.1% per additional parts per million CO_2 in RCP4.5 and RCP8.5, i.e., the mean TE increase reviewed in ref. 33. We have also considered the possibility of unchanged TE with CO_2 concentration in view of the debate on the long-term effect of CO_2 on TE (34). Radiation use efficiency, a proxy for photosynthetic

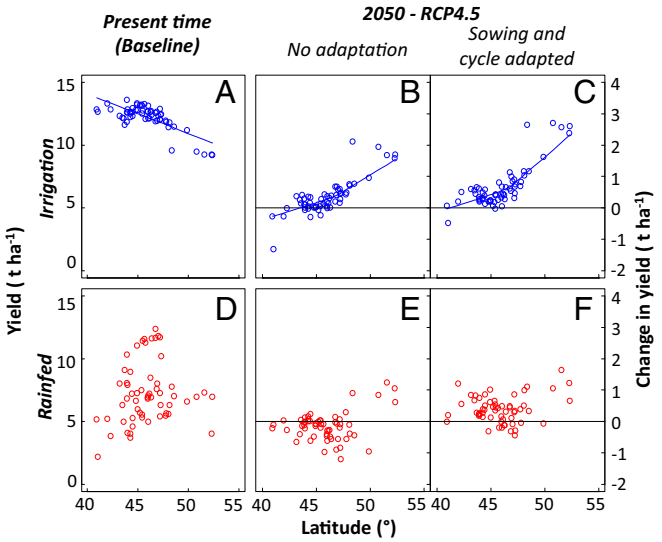

Fig. 3. Change in yield depending on farmer adaptation to climate change. (*A–D*) Current yield in irrigated and rainfed conditions. (*B*, *C*, *E*, and *F*) Change in yield between the 1975–2010 period and 2050 (RCP4.5), either without adaptation (*B* and *E*) or with adaptation of sowing date and duration of growth cycle (*C* and *F*) under irrigated (*B* and *C*) or rainfed conditions (*E* and *F*). Each point, one site, mean value for six GCMs and 30 y, calculated under the hypothesis of an increase in transpiration efficiency with CO_2 concentration.

capacity, was kept constant despite higher atmospheric CO_2 concentration because maize is a C4 species (34, 35). Simulations were run over 30 y for each combination of site, RCP, GCM, watering regime, crop cycle duration, and CO_2 effect on TE (2.6 million simulations). Climate change was represented in *SI Appendix*, Fig. S10 as sensed by plants during the optimum flowering time calculated individually for each combination of site, scenario, GCM, watering regime, and option for TE.

This resulted in increased maximum temperature, VPD, and incident light at flowering time between baseline and 2050 (*SI Appendix*, Fig. S10 *A*, *B*, and *E*), with values that were similar for RCP8.5 and RCP4.5 because flowering time was earlier in the season for RCP8.5, thereby compensating for the limited difference in temperature between RCPs at a common date. For the same reason, water deficit during flowering time was similar in 2050 compared with the baseline period 1975–2010 if TE was considered as unchanged because the earlier flowering time compensated for the negative effect of VPD increase (*SI Appendix*, Fig. S10*D*). It tended to become milder in 2050 if TE increased with atmospheric CO_2 concentration (33) because the increase in TE with CO_2 concentration reduced water use (*SI Appendix*, Fig. S10*C*).

As in previous climate impact studies, a decrease in yield was simulated in rainfed fields between the baseline period and 2050 under the hypothesis of unchanged varieties and sowing dates (RCP4.5), with a negative effect in 70% of rainfed fields (Fig. 3*D*). This negative effect was maximum at latitudes 43–47° N that represent the major growing area for maize. Conversely, simulated yields tended to increase in well-watered fields at latitudes higher than 47° N due to increased light intensity around flowering time (*SI Appendix*, Fig. S10*F*). Overall, upscaling these results for Europe as a whole across latitudes resulted in a small effect on overall production in rainfed fields (−2% and +0.6% for RCP4.5 and RCP8.5, respectively) (Fig. 4), with high negative effects in two GCMs out of six (*SI Appendix*, Fig. S11). Irrigated fields had a yield slightly increased or decreased depending on GCMs (mean, +1.8% and +1.0% for RCP4.5 and RCP8.5, respectively). Yields, weighted for the proportion of irrigated/rainfed maize in the Eurostat 25 × 25 km grid cell (*SI Appendix*, Table S1), were nearly unaffected in 2050 compared with baseline (mean, −0.8% and +0.8% for RCP4.5 and RCP8.5, respectively) if TE was considered as changing with CO_2 concentration. They were more affected if TE was considered constant in our simulations, due to more frequent water deficit, or if restrictions of water availability reduced the current portion of land area under irrigation (36).

The projected impact of climate change became positive if one assumed that farmers will adapt cycle duration and sowing date by using the decision rules they currently follow (Fig. 4). Optimal sowing dates were earlier by 10–39 d depending on sites in 2050 under RCP4.5 compared with the baseline period (*SI Appendix*, Fig. S12*A*). The cycle duration of adapted varieties increased by 207 °Cd (degree days) for RCP4.5 in irrigated fields at high latitudes (>49°), corresponding to an increase in leaf number by 3.4 (Fig. 2 and *SI Appendix*, Figs. S6 and S12). This increase disappeared in irrigated southern fields and in rainfed conditions because optimum durations were limited by the probability of negative effects of drought or heat stresses with later flowering time. If farmers followed these decision rules in 2050, the simulated impact of climate change would be positive in irrigated fields in RCP4.5 and RCP8.5, (Fig. 4*A*), regardless of hypotheses on TE and GCMs (*SI Appendix*, Figs. S11 and S13), with an effect that increased with latitude (Fig. 3*C*) and was largely accounted for by the increase in intercepted light during the crop cycle (*SI Appendix*, Fig. S14). Adapting the crop cycle duration also had a positive effect in rainfed fields (Figs. 4*B* and 3*H* and *SI Appendix*, Fig. S11 and S13), but this effect was only observed if TE was considered as increasing with CO_2 concentration and was GCM dependent. Overall, if the effect of climate change was

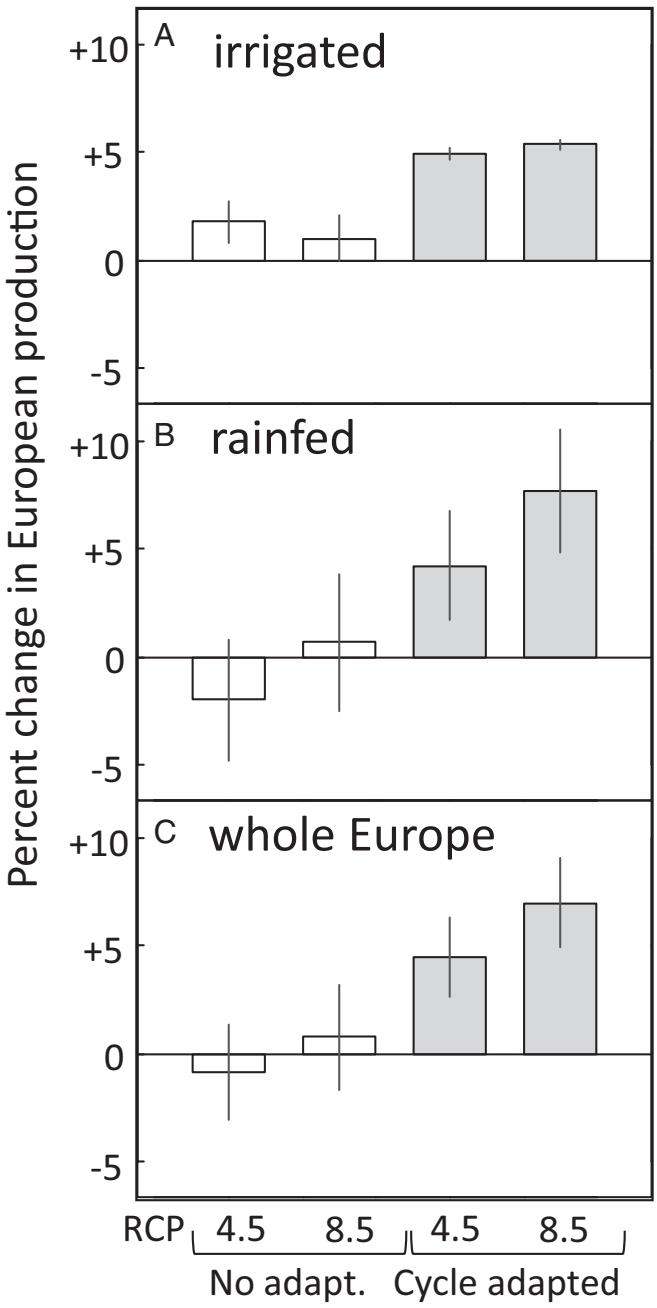

Fig. 4. Impact of climate change on European maize production depending on farmer adaptation to climate change in well-watered conditions (*A*), rainfed conditions (*B*), or Europe as a whole (*C*). The latter calculation considered the proportion of irrigated vs. rainfed maize fields in the Eurostat 25 × 25 km grid cells. Simulations consider that the maize area and access to water will be the same in 2050 compared with the 1975–2010 period, and the hypothesis of an increase in TE with CO_2 concentration. White, no adaptation; gray, adaptation of sowing date and cycle duration. Simulations for individual GCMs, with or without change in TE, are in *SI Appendix*, Fig. S11. Error bars, SE calculated over the six considered GCMs.

synthesized by weighing irrigated and rainfed fields over Europe, the total maize production increased by 4.5% and 7.0% for RCP 4.5 and 8.5, respectively, if the crop cycle was adapted, in the likely hypothesis of a moderate increase in TE.

The combined effects of climate change and of adaptation of crop cycle duration were much larger in northern than in southern locations (Fig. 3 *C*–*F*). The gradient of yield, of 0.31 t ha^{-1} per

AGRICULTURAL SCIENCES

degree of latitude for the baseline period (Fig. 3*A*) decreased to 0.09 t ha^{-1} per degree in 2050 (RCP4.5). The current north–south difference in yield in the absence of stress was therefore largely decreased by the combined effects of climate change and adaptation practices (Fig. 3 *C*–*F*).

Discussion

The approach used here to predict the impact of climate change on yield differs from those previously published, which led to contrasting results ranging from steep decrease to appreciable gains of yield (1–6, 10–12, 14). Here, we have considered adaptation via one biological process, the use of the observed genetic variability of flowering time, and explicit management practices, sowing date, and irrigation, considered with rules that mimic those currently used by farmers. This was in the line of Lobell (8) who considered it essential to precisely identify the actions (adaptation) that affect the impact of climate change and of Rezaei et al. (37) who proposed that climate change impacts should not rely on a single-cultivar concept. Furthermore, we have based our approach on experimental evidences for evaluating the effect on yield of the genetic variability of flowering time and on comparisons with historical data for testing the farmer's decision rules used in crop simulations. This has also required an improved crop simulation model that can predict the effect of the genetic variability of phenology and of responses to environmental conditions on leaf growth, grain set, and transpiration (26, 27), together with advanced phenotyping techniques for establishing the model (38). We believe that this represents progress, compared with studies that use current trends of temperature effect together with nonexplicit hypotheses on adaptation possibilities (10–12, 39).

Are farmers likely to use the genetic variability of flowering time and to adapt sowing dates by 2050? We can consider this hypothesis as reasonable because (*i*) genetic resources and alleles for adapting crop cycle duration have been identified and are increasingly available (16); and (*ii*) farmers have already adapted maize varieties in recent years, as they have done for wheat in the United States for over a century (40). For example, varieties of the group midearliness dent lines were mostly grown in France at latitudes of 44.8–45.9° in 1996 while they have shifted to 46.5–47.5° in 2009 (41). The same tendency for farmers to increasingly use late-maturing cultivars has also been observed in other species such as winter rapeseed and rye, thereby partly or fully compensating for the decrease in cycle duration linked to the increase in temperature (42).

Hence, the effect of climate change on yield might be more positive than previously reported (3–6). This particularly concerns northern areas where yield increases are maximum. However, resulting increases presented here will not be sufficient to meet the increasing demands for food and industrial usages (43). Further improvements of plant performance based on increased photosynthesis, adapted reproductive development, or resistance to pests and diseases will be necessary. Southern fields will have less of a competitive advantage in both irrigated and rain-fed conditions (Fig. 3 *D*–*H*), whereas farmers in northern areas will have the option of growing maize with high yields. This may change the maize growing area, in such a way that the positive impact of climate change on European maize production might be higher than predicted here.

Material and Methods

Field Experiments. We tested a panel of 121 maize accessions representative of main components of the maize genetic diversity (36) in three experimental fields with two watering regimes each. Sites included a Mediterranean field, Mauguio [43°36′37″N; 3°58′39″E; 23 m above sea level (asl)], and oceanic sites in Sainte Pexine (46°33′43″N; 1°08′17″W; 45 m asl) and Le Magneraud (46°24′16″N; 00°04′45″E; 26 m asl). In each site, two water regimes were imposed, with either irrigation over the crop cycle or restricted irrigation with soil water deficit at flowering time. A rainout shelter was used in Le Magneraud to ensure water deficit so the number of accessions was 57 because of the limited available space. Irrigation was withdrawn at the eight-visible-leaf stage, until flowering time plus 10 d but was still applied when plants showed leaf rolling in early morning for 2 consecutive days. The experimental design was an alpha lattice with two replicates in the irrigated treatments and three replicates in rain-fed treatments. Plots were 6 m long, with 0.8 m between rows and a plant density of 8 m^{-2}. Light, air temperature, relative humidity, and wind speed were measured every hour in each experiment at 2-m height over a reference grass canopy. Soil water potential was measured every day at 30-, 60-, and 90-cm depths in watered and rain-fed plots with three and two replicates, respectively. Mean soil water potential was −0.3 MPa on average during water deficit in Sainte Pexine and Le Magneraud, and was −0.6 MPa in Mauguio. Thermal time was calculated from sowing time as in APSIM maize (25) at a 3-h time step.

Emergence, flowering time, yield, and yield components were assessed at plot level. The length and width of every second leaf and leaf number were measured in 10 plants per plot. The leaf appearance rate of each accession was calculated by dividing the mean thermal time at flowering time by the final number of leaves of the studied accession. The duration of the vegetative period was expressed as final leaf number in Fig. 1 and *SI Appendix*, Figs. S2 and S3. We then averaged data for accessions with common final leaf number. Leaf area and light interception were calculated every day from sowing to harvest for all accessions. For that, profiles of final leaf length and width for each variety with final leaf number from 11 to 25 were obtained from measured data. The time of appearance of each leaf was calculated from the phyllochron. Leaf expansion was considered linear during 10 d from leaf appearance (27). Light interception was then calculated by using measured incident light and the proportion of intercepted light calculated from leaf area as in APSIM maize (25).

Model Parameterization and Evaluation.

Crop parameters and varieties. We used the model APSIM maize (25) modified for expansion of individual leaves (26) and calibrated (in particular for responses to water deficit and VPD) with data of the reference hybrid B73xUH007 in replicated field experiments in Mauguio, France (24) and in the phenotyping platforms PhenoArch and Phenodyn (https://www6.montpellier.inra.fr/lepse/M3P). Temperature at 3-h time step was calculated from daily minimum and maximum temperatures with the third order polynomial function used in APSIM maize (25). VPD was calculated for each 3-h time step based on current temperature and daily minimum temperature, an estimate for dew-point temperature. Leaf expansion rate was calculated every third hour, based on values VPD and soil water status with parameters as in ref. 27. The parameter representing TE before correction by the effect of VPD (parameter transp_eff_cf in APSIM maize) was set at 0.0075 g kPa g^{-1} for the baseline period and increased by 0.1% per additional μmol CO_2 mol^{-1} resulting in +11% and 17% in 2050 for RCP4.5 and RCP8.5, respectively (33).

A set of virtual hybrids with contrasted crop cycle durations was derived from the reference hybrid, in which crop cycle duration depended on the duration of the vegetative stage. The duration of the vegetative period was driven by the final leaf number (ref. 22 and *SI Appendix*, Fig. S2). We parameterized hybrids with contrasted cycle duration by (*i*) changing leaf number from 11 to 30, with a constant leaf appearance of 0.0193 °Cd $leaf^{-1}$ for all accessions (*SI Appendix*, Fig. S2) and (*ii*) a constant thermal time from flowering to maturity corresponding to the reference hybrid. The durations of each phenological stage of the vegetative period were affected proportionally to changes in time from emergence to flowering. All other parameters were those of the reference hybrid (24). Hence, the 16-leaf hybrid was the reference hybrid and hybrids with leaf number ranging from 11 to 30 were similar to the reference hybrid but with different final leaf number.

Sites. We used 59 locations representative of the European maize growing area and of typical soil types of these regions. Fifty-five sites were those described previously (24), representing the 10 European countries with the highest maize growing areas in the 2004–2009 period (30) and the main maize growing regions within these countries (24). Four sites were added to improve the spatial distribution of locations. Soil data were obtained from the Joint Research Centre (JRC) European Soil Commission database and from the Crop Growth Monitoring System (24). Because soil depth can highly vary within each region and because the aim of this study was a sensitivity analysis on other variables, we considered a soil depth of 1.5 m in all sites. Meteorological data used for the baseline period were 36 y of daily weather (1975–2010) obtained from (*i*) the AGRI4CAST database of the JRC for the 55 sites (24) and (*ii*) the INRA CLIMATIK database for the four added sites. The atmospheric CO_2 concentration was 380 ppm. For comparing predicted and observed current European yields, plant density and nitrogen supply were adjusted for each site based on the JRC database* and local knowledge. Because there is no reason to hypothesize that these values will stay the

*JRC (2013) JRC database crop knowledge. ed JRC (Joint Research Centre, Ispra, Italy).

same in 2050, common sowing density of eight plants m^{-2} and no nitrogen limitation were used in the final set of simulations to compare the baseline period and future climate scenarios.

Modeling sowing and harvesting dates. Sowing dates were simulated in each field as the first day from January to May in which the frequency of frost was <5% in the following 10 d (calculated over 36 y in each site). The same rule was used for the 2050 climate scenarios. Harvest date was simulated as occurring after physiological maturity, on the first day when soil water content of the 0- to 30-cm top layer was below 90% saturation. The latter rule simulated the impossibility for harvester machines to enter into the considered field because of an insufficient load-bearing capacity. The model simulated a total yield loss if harvest could not happen before November 1, due to the high risk of ear fall and diseases, combined with the necessity for farmers to sow the next winter crop at that time.

Two watering regimes were simulated in each site, either rainfed or with systematic watering until field capacity over the entire soil profile every 3rd day. The optimums for each of these cultivation practices were calculated for each combination of site, year, scenario, GCM, watering regime, and option for TE. In simulations, we considered one single optimum for all studied years, simulating the fact that farmers can estimate frequencies at each site but cannot forecast climatic conditions for adjusting decisions to individual years.

Simulations and upscaling. The climate scenarios in 2050 were simulated at each site by using the stochastic weather generator LARS-WG (32) and were based on climate projections from the CMIP5 ensemble with RCPs 4.5 and 8.5 (487 and 541 ppm CO_2 in 2050, respectively) and six GCMs, namely GFDL-CM3, HadGEM2-ES, MIROC5, MPI-ESM-MR, CMCC-CM, and MIROC-ESM. The respective positions of these GCMs are compared in *SI Appendix*, Fig. S9 to 18 GCMs from the CMIP5 ensemble in terms of changes in precipitation, VPD, relative humidity, and in mean temperature calculated over land in Northern and Southern Europe. In Southern Europe, GFDL-CM3 is the hottest and nearly the driest GCM from the CMIP5 ensemble. One-hundred years of daily weather data were generated for each combination of site, RCP, and GCM.

A total of 2,897,136 crop simulations were run (for the baseline period: 2 managements × 2 irrigations scenarios × 31 accessions × 59 sites × 36 y; for climate scenarios: 2 scenarios × 6 GCMs × 2 irrigations scenarios × 31 accessions × 59 sites × 30 y × 2 options for TE). To upscale results from sites to each country, simulated data under full-irrigation and rainfed scenarios were weighted for each site by the proportion of irrigated maize fields in the area from the JRC database, data originally from Siebert et al. (36) (*SI Appendix*, Table S1). Results were then averaged at country level. To upscale to European level, results at country levels were multiplied by the area of maize cultivation in each site, based on the 25 × 25 km grid cell of the Eurostat database on year 2010.

ACKNOWLEDGMENTS. We thank Josiane Lorgeou (Arvalis) and Brigitte Gouesnard (INRA) for their contributions to the experiments. This work was supported by the European project FP7-244374 (DROPS), and the Agence Nationale de la Recherche projects ANR-10-BTBR-01 (Amaizing) and ANR-11-INBS-0012 (Phenome). Rothamsted Research receives strategic funding from the Biotechnology and Biological Sciences Research Council.

1. Asseng S, et al. (2015) Rising temperatures reduce global wheat production. *Nat Clim Chang* 5:143–147.
2. Cammarano D, et al. (2016) Using historical climate observations to understand future climate change crop yield impacts in the Southeastern US. *Clim Change* 134:311–326.
3. Xu H, Twine TE, Girvetz E (2016) Climate change and maize yield in Iowa. *PLoS One* 11:e0156083.
4. Yang CY, Fraga H, Van Ieperen W, Santos JA (2017) Assessment of irrigated maize yield response to climate change scenarios in Portugal. *Agric Water Manage* 184:178–190.
5. Zhang Y, Zhao YX, Chen SN, Guo JP, Wang EL (2015) Prediction of maize yield response to climate change with climate and crop model uncertainties. *J Appl Meteorol Climatol* 54:785–794.
6. Urban DW, Sheffield J, Lobell DB (2015) The impacts of future climate and carbon dioxide changes on the average and variability of US maize yields under two emission scenarios. *Environ Res Lett* 10:045003.
7. Fischer EM, Knutti R (2012) Robust projections of combined humidity and temperature extremes. *Nat Clim Chang* 3:126–130.
8. Lobell DB (2014) Climate change adaptation in crop production: Beware of illusions. *Global Food Secur* 3:72–76.
9. Moore FC, Lobell DB (2015) The fingerprint of climate trends on European crop yields. *Proc Natl Acad Sci USA* 112:2670–2675.
10. Butler EE, Huybers P (2013) Adaptation of US maize to temperature variations. *Nat Clim Chang* 3:68–72.
11. Challinor AJ, et al. (2014) A meta-analysis of crop yield under climate change and adaptation. *Nat Clim Chang* 4:287–291.
12. Moore FC, Lobell DB (2014) Adaptation potential of European agriculture in response to climate change. *Nat Clim Chang* 4:610–614.
13. White JW, Hoogenboom G, Kimball BA, Wall GW (2011) Methodologies for simulating impacts of climate change on crop production. *Field Crops Res* 124:357–368.
14. Zimmermann A, et al. (2017) Climate change impacts on crop yields, land use and environment in response to crop sowing dates and thermal time requirements. *Agric Syst* 157:81–92.
15. Bouchet S, et al. (2013) Adaptation of maize to temperate climates: Mid-density genome-wide association genetics and diversity patterns reveal key genomic regions, with a major contribution of the Vgt2 (ZCN8) locus. *PLoS One* 8:e71377.
16. Buckler ES, et al. (2009) The genetic architecture of maize flowering time. *Science* 325:714–718.
17. Romero Navarro JA, et al. (2017) A study of allelic diversity underlying flowering-time adaptation in maize landraces. *Nat Genet* 49:476–480.
18. Salvi S, et al. (2007) Conserved noncoding genomic sequences associated with a flowering-time quantitative trait locus in maize. *Proc Natl Acad Sci USA* 104:11376–11381.
19. Zheng B, Chenu K, Fernanda Dreccer M, Chapman SC (2012) Breeding for the future: What are the potential impacts of future frost and heat events on sowing and flowering time requirements for Australian bread wheat (Triticum aestivum) varieties? *Glob Chang Biol* 18:2899–2914.
20. Debieu M, et al. (2013) Co-variation between seed dormancy, growth rate and flowering time changes with latitude in Arabidopsis thaliana. *PLoS One* 8:e61075.
21. Li YX, et al. (2016) Identification of genetic variants associated with maize flowering time using an extremely large multi-genetic background population. *Plant J* 86:391–402.
22. Li D, et al. (2016) The genetic architecture of leaf number and its genetic relationship to flowering time in maize. *New Phytol* 210:256–268.
23. Tardieu F (2012) Any trait or trait-related allele can confer drought tolerance: Just design the right drought scenario. *J Exp Bot* 63:25–31.
24. Harrison MT, Tardieu F, Dong Z, Messina CD, Hammer GL (2014) Characterizing drought stress and trait influence on maize yield under current and future conditions. *Glob Chang Biol* 20:867–878.
25. Hammer GL, et al. (2010) Adapting APSIM to model the physiology and genetics of complex adaptive traits in field crops. *J Exp Bot* 61:2185–2202.
26. Chenu K, et al. (2008) Short-term responses of leaf growth rate to water deficit scale up to whole-plant and crop levels: An integrated modelling approach in maize. *Plant Cell Environ* 31:378–391.
27. Lacube S, et al. (2017) Distinct controls of leaf widening and elongation by light and evaporative demand in maize. *Plant Cell Environ* 40:2017–2028.
28. IPCC (2007) Autonomous adaptions. *Climate Change 2007: Impacts, Adaptation, and Vulnerability*. Contribution of Working Group II to the Fourth Assessment Report of the Intergovernmental Panel on Climate Change, eds Parry M, Canziani O, Palutikof J, van der Linden P, Hanson C (Cambridge Univ Press, New York).
29. JRC, IES, MARS (2015) JRC Database Agri4cast 2015-1.0. ed JRC (Joint Research Centre, Ispra, Italy). Available at agri4cast.jrc.ec.europa.eu/DataPortal/Index.aspx. Accessed November, 2016.
30. JRC (2016) European commission. Eurostat database. Available at ec.europa.eu/eurostat/web/agriculture/data/database. Accessed November, 2016.
31. Semenov MA, Stratonovitch P (2010) Use of multi-model ensembles from global climate models for assessment of climate change impacts. *Clim Res* 41:1–14.
32. Semenov MA, Stratonovitch P (2015) Adapting wheat ideotypes for climate change: Accounting for uncertainties in CMIP5 climate projections. *Clim Res* 65:123–139.
33. Lobell DB, et al. (2015) The shifting influence of drought and heat stress for crops in northeast Australia. *Glob Chang Biol* 21:4115–4127.
34. Kimball BA (2016) Crop responses to elevated CO2 and interactions with H2O, N, and temperature. *Curr Opin Plant Biol* 31:36–43.
35. Kim SH, et al. (2006) Canopy photosynthesis, evapotranspiration, leaf nitrogen, and transcription profiles of maize in response to CO2 enrichment. *Glob Chang Biol* 12:588–600.
36. Siebert S, et al. (2005) Development and validation of the global map of irrigation areas. *Hydrol Earth Syst Sci* 9:535–547.
37. Rezaei EE, Siebert S, Hüging H, Ewert F (2018) Climate change effect on wheat phenology depends on cultivar change. *Sci Rep* 8:4891.
38. Tardieu F, Cabrera-Bosquet L, Pridmore T, Bennett M (2017) Plant phenomics, from sensors to knowledge. *Curr Biol* 27:R770–R783.
39. Challinor AJ, Koehler AK, Ramirez-Villegas J, Whitfield S, Das B (2016) Current warming will reduce yields unless maize breeding and seed systems adapt immediately. *Nat Clim Chang* 6:954–958.
40. Olmstead AL, Rhode PW (2011) Adapting North American wheat production to climatic challenges, 1839-2009. *Proc Natl Acad Sci USA* 108:480–485.
41. Arvalis (2016) Choisir et Decider. Préconisations régionales 2016. Available at https://www.arvalis-infos.fr/file/galleryelement/pj/1c/49/26/b7/choisirmais2016_aquitaine_midipyrenees3339212978836866791.pdf. Accessed November, 2017.
42. Rezaei EE, Siebert S, Ewert F (2017) Climate and management interaction cause diverse crop phenology trends. *Agric For Meteorol* 233:55–70.
43. IPCC (2014) Summary for policymakers. *Climate Change 2014: Impacts, Adaptation, and Vulnerability. Part A: Global and Sectoral Aspects*. Contribution of Working Group II to the Fifth Assessment Report of the Intergovernmental Panel on Climate Change, eds Field CB, etc. (Cambridge Univ Press, New York), pp 1–32.